Feasibility of N2 Binding and Reduction to Ammonia on Fe-Deposited MoS2 2D Sheets: A DFT Study

Feasibility of N_2 binding and reduction into ammonia at Fe-deposited-on MoS_2 2D sheets: A DFT study

Luis Miguel Azofra,*[a] Chenghua Sun,[b] Luigi Cavallo,[a] and Douglas R. MacFarlane*[b]

Abstract: Based on the structure of the nitrogenase FeMo cofactor (FeMoco), we show that Fe-deposited-on MoS_2 2D sheet exhibits high selectivity towards spontaneous fixation of N_2 against chemisorption of CO_2 and H_2O. Our DFT predictions also indicate the ability of this material to convert N_2 into NH_3 with maximum energy input of 1.02 eV as an activation barrier for the first proton-electron pair transfer.

Introduction

In a changing world that demands real alternatives to non-renewable energy sources based on oil, ammonia (NH_3) is recently being considered as a 'green fuel'[1] which does not compromise on environmental sustainability. Since the major source for NH_3 synthesis is atmospheric dinitrogen (N_2), NH_3 utilisation produces a zero-balance of greenhouse emissions. Together with dihydrogen (H_2), NH_3 is profiled as an eco-friendly energy store for a sustainable energy future. However, synthesis of NH_3 at industrial scale exhibits serious limitations due to the complex and considerable plant infrastructure that the Haber–Bosch process requires, in addition to the intense conditions of pressure (□15–25 MPa) and temperature (□400–500 °C),[2] making it logistically inefficient in terms of transportation and distribution. To address this requires alternative routes for NH_3 synthesis under mild conditions; in recent years, the (photo)[3]-electrochemical catalytic approach[4] has been of great interest, because it has provided the first steps towards the development of an efficient technology for NH_3 synthesis at remote, high solar insolation areas where renewable energy can be readily generated.

Molybdenum disulphide (MoS_2) is a 2D graphene-like material that has attracted growing interest because of its chemical stability, semiconductor properties (indirect band gap of ~1.7 eV for bulk 2H-MoS_2),[5] and catalytic properties. It exists in two main crystalline phases, the thermodynamically stable 2H phase and the metastable 1T phase. It has been shown to be an efficient, viable material for heterogeneous catalysis of the hydrogen evolution reaction (HER),[6] or, in some remarkable cases, as a robust carbon dioxide (CO_2) conversion and HER catalyst through the Mo-terminated edges.[7]

As far as we know, no catalytic prospects for basal and more abundant planes of 2H-MoS_2 have been reported in the literature concerning the conversion of atmospheric gases such as H_2O [in the oxygen evolution (OER) or hydrogen evolution reactions] or CO_2. Doping with different transition metals may result in a different scenario, in which modifications to the structure-reactivity pattern may improve the reduction activity, as recently proposed by Xiao *et al*. for OER[8] and Nørskov and co-workers for HER[9] and CO_2 electro-reduction.[10] Other novel structures for transition metal catalysts include the suspension of Fe clusters on graphene pores[11] and, more recently, Fe nanoparticle (~3 nm in size) arrays on MoS_2.[12] These efforts open new possibilities for application of these materials as selective catalytic materials. Generally, however, while many advances have been made for CO_2 capture and conversion,[13] the search for efficient materials for selective N_2 reduction is still at a preliminary stage.

Recently, Neese and co-workers[14] provided X-ray emission spectroscopy evidence for a definitive structure of the nitrogenase FeMo cofactor (FeMoco), **Fig. 1**, indicating that the cluster contains a central C^{4-} atom. As stated by MacLeod and Holland,[15] the FeMo active site of nitrogenase enzymes is a source of inspiration for Fe- and/or Mo-based catalysts capable of fixing, even reducing N_2 into NH_3;[16] however, most previous attempts to mimic this enzyme have been for homogeneous catalysis, while our objective is to search for heterogeneous electrocatalysts for active N_2 capture and conversion.

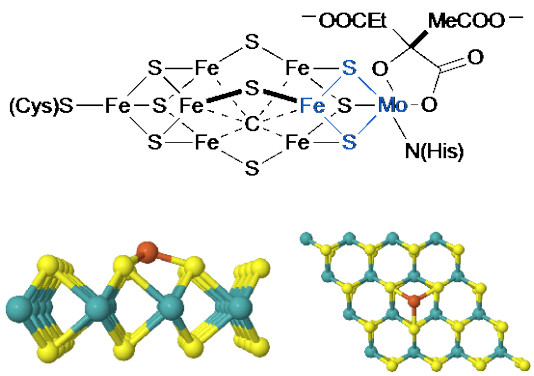

Figure 1. Kekulé representation of nitrogenase FeMo cofactor and optimised Fe-deposited-on 4×4 MoS_2 2D sheet (side and top views).

[a] Dr. L. M. Azofra, Prof. Dr. L. Cavallo
KAUST Catalysis Center (KCC)
King Abdullah University of Science and Technology (KAUST)
Thuwal 23955-6900, Saudi Arabia
Email: luis.azoframesa@kaust.edu.sa
[b] Dr. C. Sun, Prof. Dr. D. R. MacFarlane
ARC Centre of Excellence for Electromaterials Science (ACES)
School of Chemistry, Faculty of Science, Monash University
Clayton, VIC 3800, Australia
Email: Douglas.MacFarlane@monash.edu

Supporting Information for this article contains: thermochemistry details, computation of activation barriers in electrochemical reactions, computational settings, Gibbs free energies, and optimised structures leading to unambiguous reproducibility of the present outcomes.

In the present work we show that, using DFT, an absolutely inactive material for N_2 conversion (2H-MoS_2) becomes active for this purpose when single Fe atoms are deposited on the basal planes, thereby mimicking FeMoco. The modified material is also calculated to spontaneously and selectively capture N_2, relative to H_2O or CO_2 fixation. Thus, using well-resolved DFT calculations, we investigate the mechanism of N_2 capture and electrochemical conversion into NH_3 catalysed by single-atom Fe deposited on 2H-MoS_2. Our calculations examine the thermodynamics that govern this process, and also estimate the activation barriers (kinetics)[17] that emerge in the form of over-potentials for this specific catalyst. Accurate calculation of over-potentials is a current challenge for DFT, but is critical for experimentalists to make full use of the calculated results.

Computational Details

The mechanism for the capture of N_2 and its electrochemical conversion into NH_3 catalysed by Fe-deposited-on 2H-MoS_2 2D sheet has been studied by means of density functional theory (DFT) through the generalised gradient approximation (GGA) with the Perdew–Burke–Ernzerhof (PBE) functional,[18] using a plane-wave cut-off energy of 450 eV,[19] and representative Fe-deposited 4×4 MoS_2 (Fe:$Mo_{16}S_{32}$) super-cells. The Brillouin zone (periodic boundary conditions) was sampled by 3×3×1 k-points using the Monkhorst–Pack scheme. In order to avoid interactions between periodic images, a vacuum distance of 20 Å was imposed between different layers. Optimisation calculations were done using energy and force convergence limits equal to 10^{-4} eV/atom and |0.05| eV/Å, respectively. Thermal and zero point energy (ZPE) corrections were calculated over Γ points. Also, explicit dispersion correction terms to the energy were employed through the use of the D3 method with the standard parameters programmed by Grimme and co-workers.[20] The nudge elastic band (NEB) method[21] has been applied in order to locate the transition states (TS) through the minimum energy path. With exception of the energy and force convergence limits (10^{-3} eV/atom, |0.10| eV/Å), similar computational settings have been applied as to the location of minima and intermediate states. Also, charge analysis has been performed through the Bader's approach in 3×3 MoS_2 super-cells, in which the atomic surfaces are divided by the location of minima of charge density perpendicular to them (the so-called zero flux surfaces).[22]

Finally, density of states profiles (DOS) for bulk 2H-MoS_2 and Fe-deposited-on MoS_2 2D sheets, they have been calculated at the Heyd–Scuseria–Ernzerhof (HSE06) functional[23] level (single point) over the optimised PBE structures. Band gap for reference bulk 2H-MoS_2 is very well predicted (1.73 eV). The presence of Fe as a deposited metal on MoS_2 is characterised by the appearance of two states beyond and below the conductive and valence bands, respectively, with a still semiconductor behaviour and an approximate band gap of 0.65 eV.

All optimisation and vibrational frequency calculations have been performed throughout the facilities provided by the Vienna *Ab-Initio* Simulation Package (VASP, version 5.3.5).[24]

All Gibbs free energy values for the N_2 reduction mechanism are referred to the computational hydrogen electrode (CHE) model using the proton-coupled electron transfer (PCET) approach.[25] Use of this model is clearly approximation since it is possible that the electron transport is not full coupled to the proton transfer. However, methodology to deal with the activation barriers in the latter situation has not yet been developed. This PCET approach considers the chemical potential of the H^+/e^- pair in aqueous solution as half of the H_2 gas molecule at standard hydrogen electrode (SHE) conditions, *i.e.*, $f(H_2)$ = 101 325 Pa and U = 0 V, being $f(H_2)$ and U the fugacity of H_2 and the external potential applied, respectively. [At pH = 0, this corresponds to the normal hydrogen electrode (NHE) reference scale; full thermochemistry details at the Supporting Information]. Both, binding and reaction/activation Gibbs free energies have been calculated at mild conditions of temperature, T = 298.15 K.

Results and Discussion

N_2 binding

As shown in **Fig. 1**, when a single Fe metal atom is deposited on one of the naked basal planes of MoS_2, this leads to the formation of three four-membered FeSMoS rings. The Fe is strongly bound, with interatomic Fe–S distances of 2.05 Å and binding energy of –4.28 eV. This structural motif is extremely close to that of the FeMo active site of nitrogenase FeMoco (highlighted in blue in **Fig. 1**). However, while Harris and Szilagyi[26] hypothesised that the oxidation state of Fe moieties in FeMoco are 2Fe(II) + 5Fe(III) in the presence of a homocitrate ligand, one might expect that Fe is of lower oxidation state when deposited as Fe(0) on a MoS_2 surface. Through Bader charge analysis, it can be seen that the charges of the three sulphur

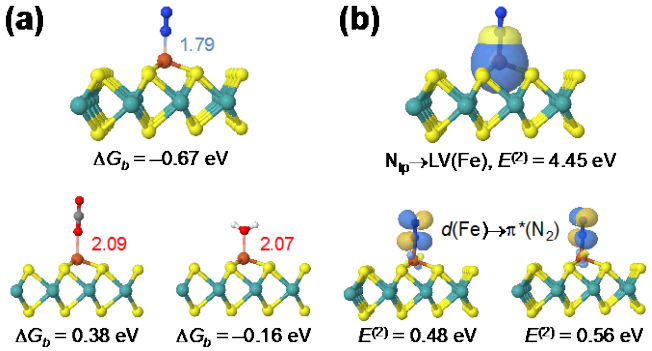

Figure 2. (a) Chemisorbed N_2, CO_2, and H_2O minima. Proximal $d_{Fe–N/O}$ distances (in Å) are indicated in blue and red, respectively. Gibbs free binding energies, ΔG_b, at mild conditions (T = 298.15 K, f = 101 325 Pa). **(b)** Pre-normalised NBO corresponding to the N_{lp}→LV(Fe) and d(Fe)→π*(N_2) interactions in the N_2 chemisorbed species on the Fe-deposited-on MoS_2 surface.

atoms directly interacting with Fe increase by around 0.17 e per atom compared with the non-decorated MoS_2 material. Vicinal Mo atoms to them and the rest of the S atoms also exhibit increments of charge, although lower in magnitude, while the rest of the Mo centres, small depletions of charge varying between 0.04-0.08 e can be seen. This transfer of charge from Fe to MoS_2 results in a net charge on Fe of around +0.8.

The first consequence of this is seen in **Fig. 2(a)**. The electropositive charge of Fe on MoS_2 makes this centre a plausible binding site for negative entities from partner molecules, such as lone pairs on N_2, CO_2, or H_2O. The N_2 fixation is hypothesised to be spontaneous, with a binding Gibbs free energy of –0.67 eV and an interatomic N–Fe distance of 1.79 Å. In contrast, CO_2 fixation is a non-spontaneous process (0.38 eV) on Fe, while capture of H_2O (ΔG_b = –0.16 eV) is not as favourable as N_2 fixation. Undoubtedly, this suggests promising prospects for the testing of this material in an aqueous environment.

The nature of the N–Fe interaction, which is around three times more intense than the H_2O–Fe interaction, can be explained from the natural bonding orbital (NBO) perspective.[27] NBO analysis over the Γ point in the chemisorbed N_2 state [**Fig. 2(b)**] suggests that a strong N_{lp}→LV(Fe) charge transfer is taking place between the N_2 lone pair and the 'lone vacant' orbital in Fe as a σ-bonding interaction with $E^{(2)}$ = 4.45 eV. Complementarily, *d* orbitals at Fe back-donate to the π* at N_2 throughout two main *d*(Fe)→ π*(N_2) charge transfers with $E^{(2)}$ NBO interaction energies accounting, in sum, in 1.04 eV. Consequently, N≡N bond elongation occurs: from 1.098 Å in the gas-phase equilibrium to 1.14 Å once fixed on the Fe-deposited-on the MoS_2 surface.

As shown in **Fig. 3(a)**, supplementary 2 ps NVT molecular dynamics calculations clearly indicate the stability of the Fe–S bonds in the presence of a H_2O monolayer at room temperature. DOS profiles for pure and Fe-deposited-on-MoS_2 have been calculated, as shown in **Fig. 3(b)**, in which additional occupied and unoccupied states close to the Fermi level have been introduced by the Fe deposition. As Fe is introduced to the surface through three Fe–S bonds, a tetrahedral crystal-splitting field is generated, meaning that electrons from N_2 can fill the unoccupied t_2 orbitals of the Fe centre. This suggests that N_2 is not only effectively captured, but also activated by the proposed electron transfer. In principle, strong physicochemical contact between the catalyst surface (Fe-deposited-on MoS_2) and N_2 gas is essential for room-temperature N_2 conversion; otherwise, extensive energy input or high pressure is needed.

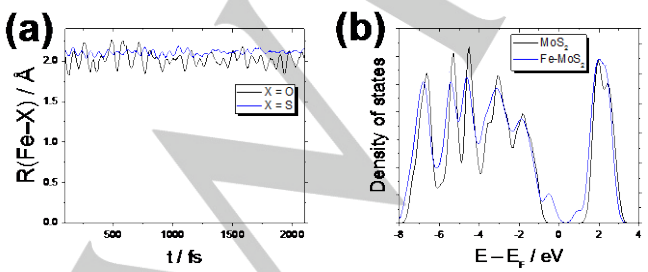

Figure 3. (a) Fe–O and Fe–S distance variations during 2 ps NVT molecular dynamics in the presence of a water monolayer. **(b)** DOS profile for MoS_2 and Fe-deposited-on MoS_2 2D sheets.

N_2 conversion into NH_3

Recent investigations carried out by us on 'MXenes' as potential catalysts for N_2 reduction into NH_3[28] suggested that, as occurs with the electrochemical conversion of CO_2 into hydrocarbon compounds,[29] the first hydrogenation step is usually the limiting step for the whole reaction, from both the thermodynamic and kinetics points-of-view. In the present case, our DFT results imply that the first H^+/e^- pair transfer on the chemisorbed N_2 state, which leads to the chemisorbed NNH• radical, is produced *via* a non-spontaneous process, requiring 0.99 eV. This energy value only includes the thermodynamic cost for the first elementary reduction step; if kinetic effects are considered *via* the transition state barrier, the energy cost becomes 1.02 eV. [See **Fig. 4(a)**].

An in-depth investigation of the different mechanistic paths reveals that the NNH• intermediate species preferentially exists when the H moiety is placed on the farthest (or outer) N atom of the N_2 molecule with respect to the material. As can be seen in **Fig. 4(b)**, the FeNNH• motif is thermodynamically preferred over the FeNHN• one. Although obtaining NNH• seems to demand an injection of energy, it is also worth mentioning that the N–Fe bond is intensified, with the interatomic distance becoming 0.13 Å shorter than at the captured N_2 step. As it was previously analysed, Bader charge analysis indicates that, at this step, MoS_2 moiety still supports an extra charge mainly depleted from Fe and being another minor quantity given to the NNH• species, although corroborating its radical nature. Thus, q(Fe) decreases around 7 e intensifying its transition from Fe(0) to Fe(I) as consequence of its deposition (and further electron charge transfer) on MoS_2 and the chemical events taking place on it during the N_2 conversion.

Similar to the observations during the first hydrogenation stage, the second H^+/e^- pair transfer also exhibits a non-negligible activation barrier of 0.85 eV. However, while in the previous case the product exhibited a thermodynamic impediment of 0.99 eV, obtaining the NNH_2 intermediate species only requires 0.13 eV. By computing and comparing the thermodynamic stabilities of the two plausible NNH_2 and NHNH second-order reduced species, the mechanism where this second hydrogenation occurs on the previously hydrogenated centre is clearly defined.

During the third H^+/e^- pair transfer, which our DFT findings imply is a spontaneous process, a release of the first NH_3 molecule occurs, and presumably, a single N• atom remains on the surface. This chemical entity has been assumed in the literature to be a stable radical,[16d,28,30] however Bader charge analysis estimates that q(N) for this species is equal to 5.52 e (*i.e.*, a net charge of –0.52). This invites debate on whether N• is formally a radical or a distinct negative species, as a

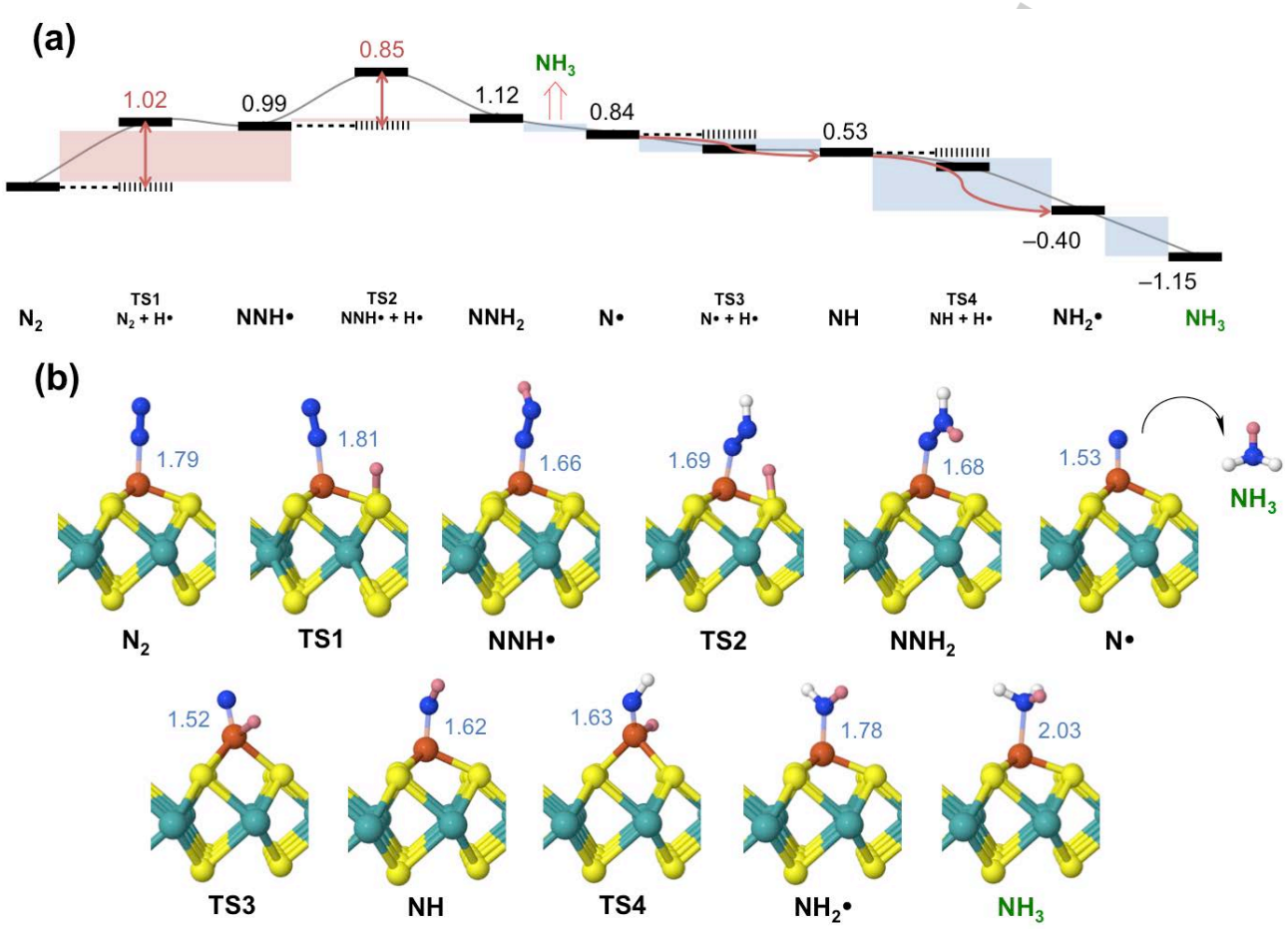

Figure 4. (a) Minimum Gibbs free energy path corresponding to N_2 conversion into NH_3 catalysed by Fe-deposited-on MoS_2 2D sheet. Gibbs free reaction (black) and activation (red) energies *vs.* CHE [$f(H_2)$ = 101 325 Pa, and U = 0 V; pH = 0], at T = 298.15 K, are shown in eV. Blue and red shadings indicate spontaneous and non-spontaneous reactive steps, respectively. **(b)** Structures of minima and transition states (TS) with selected d_{Fe-N} distances (blue) in Å. For clarity, reactive hydrogen moieties during the electrochemical N_2 conversion process are highlighted in pink.

consequence of some charge transfer from an electropositive centre such as Fe to the more electronegative N atom.

In the present work, we hypothesise that the strong electron affinity of such species facilitates the fourth, fifth, and sixth H^+/e^- pair transfers, making insertion of these new sets of H moieties "easier" in terms of activation energy. They are estimated to be barrier-less processes.[28] Also, going to the production of the second NH_3 molecule, passing through NH and NH_2• intermediate species, a cascade of spontaneous elementary reactions take place. Finally, desorption of the aforementioned second NH_3 molecule only requires 0.56 eV; however, although this extra energy should be supplied by the maximum of 1.02 V *vs.* CHE over-potential required for the first H^+/e^- pair transfer, the fixation of N_2 is favoured over that of NH_3, ensuring the continuity more electro-reduction cycles by auto-regeneration of the material.

Conclusions

In summary, a bio-inspired catalyst structure consisting of Fe-deposited-on-MoS_2 2D sheet, is characterised by an effective adsorption of N_2 through $N_{lp}\rightarrow$LV(Fe) σ-donation from N_2 to the Fe centre and complementary d(Fe)$\rightarrow \pi^*(N_2)$ π-back-donation, a spontaneous and effective process, which is favoured over the capture of CO_2 or H_2O. Bader charge analysis hypothesises that Fe centre yields electron charge to MoS_2 tending to the formation of the very rare and reactive Fe(I) species. The catalyst should catalyse conversion of N_2 into NH_3 under mild conditions; the limiting step is proposed to be the first H^+/e^- pair transfer, which has an activation barrier of 1.02 eV. In addition to the promising prospects for use in aqueous environments, the lower binding energy between NH_3 and the material compared with that for N_2 capture implies that the material will auto-regenerate, and thus can be used for successive electro-reduction cycles. We hope that this work will stimulate further interest in this research area, with important implications for energy and the environment.

Acknowledgements

LMA and LC acknowledge King Abdullah University of Science and Technology (KAUST) for support, and CS and DRM thank the Australian Research Council (ARC) for CS's Future Fellowship and DRM's Laureate Fellowship, as well as support through the ARC Centre of Excellence for Electromaterials Science. Gratitude is also due to the KAUST Supercomputing Laboratory using the supercomputer Shaheen II and the National Computational Infrastructure (NCI) for providing the computational resources.

Keywords: N_2 capture • N_2 conversion • NH_3 electro-synthesis • MoS_2 • computer-aided design

[1] R. Lan, S. Tao, *Front. Energy Res.* **2014**, *2*, 35.

[2] M. Appl, *Ammonia – Ullmann's Encyclopedia of Industrial Chemistry*, Wiley-VCH Verlag GmbH & Co. KGaA, 2002.

[3] a) T. Oshikiri, K. Ueno, H. Misawa, *Angew. Chem. Int. Ed.* **2016**, *55*, 3942–3946; b) M. Ali, F. L. Zhou, K. Chen, C. Kotzur, C. L. Xiao, L. Bourgeois, X. Y. Zhang, D. R. MacFarlane, *Nat. Commun.* **2016**, *7*, 11335.

[4] C. J. M. van der Ham, M. T. M. Koper, D. G. H. Hetterscheid, *Chem. Soc. Rev.* **2014**, *43*, 5183–5191.

[5] K. K. Kam, B. A. Parkinson, *J. Phys. Chem.* **1982**, *86*, 463–467.

[6] a) A. B. Laursen, S. Kegnæs, S. Dahl, I. Chorkendorff, *Energy Environ. Sci.* **2012**, *5*, 5577–5591; b) D. Voiry, M. Salehi, R. Silva, T. Fujita, M. Chen, T. Asefa, V. B. Shenoy, G. Eda, M. Chhowalla, *Nano Lett.* **2013**, *13*, 6222–6227.

[7] a) T. F. Jaramillo, K. P. Jørgensen, J. Bonde, J. H. Nielsen, S. Horch, I. Chorkendorff, *Science* **2007**, *317*, 100–102; b) M. Asadi, B. Kumar, A. Behranginia, B. A. Rosen, A. Baskin, N. Repnin, D. Pisasale, P. Phillips, W. Zhu, R. Haasch, R. F. Klie, P. Král, J. Abiade, A. Salehi-Khojin, *Nat. Commun.* **2014**, *5*, 4470.

[8] B. B. Xiao, P. Zhang, L. P. Han, Z. Wen, *Appl. Surf. Sci.* **2015**, *354*, 221–228.

[9] C. Tsai, K. Chan, J. K. Nørskov, F. Abild-Pedersen, *Catal. Sci. Technol.* **2015**, *5*, 246–253.

[10] X. Hong, K. Chan, C. Tsai, J. K. Nørskov, *ACS Catal.* **2016**, *6*, 4428–4437.

[11] H.-C. Hsu, C.-B. Wu, K.-L. Hsu, P.-C. Chang, T.-Y. Fu, V. R. Mudinepalli, W.-C. Lin, *Appl. Surf. Sci.* **2015**, *357*, 551–557.

[12] J. Zhao, Q. Deng, A. Bachmatiuk, G. Sandeep, A. Popov, J. Eckert, M. H. Rümmeli, *Science* **2014**, *343*, 1228–1232.

[13] a) L. Yang, H. Wang, *ChemSusChem* **2014**, *7*, 962–998; b) G. Cui, J. Wang, S. Zhang, *Chem. Soc. Rev.* **2016**, *45*, 4307–4339; c) C. Kunkel, F. Viñes, F. Illas, *Energy Environ. Sci.* **2016**, *9*, 141–144.

[14] K. M. Lancaster, M. Roemelt, P. Ettenhuber, Y. Hu, M. W. Ribbe, F. Neese, U. Bergmann, S. DeBeer, *Science* **2011**, *334*, 974–977.

[15] K. C. MacLeod, P. L. Holland, *Nature Chem.* **2013**, *5*, 559–565.

[16] a) R. R. Schrock, *Acc. Chem. Res.* **2005**, *38*, 955–962; b) M.-E. Moret, J. C. Peters, *Angew. Chem. Int. Ed.* **2011**, *50*, 2063–2067; c) K. Arashiba, Y. Miyake, Y. Nishibayashi. *Nat. Chem.* **2011**, *3*, 120–135; d) J. S. Anderson, J. Rittle, J. C. Peters, *Nature* **2013**, *501*, 84–87.

[17] X. Nie, M. R. Esopi, M. J. Janik, A. Asthagiri, *Angew. Chem. Int. Ed.* **2013**, *52*, 2459–2462.

[18] J. P. Perdew, K. Burke, M. Ernzerhof, *Phys. Rev. Lett.* **1996**, *77*, 3865–3868.

[19] a) P. E. Blöchl, *Phys. Rev. B* **1994**, *50*, 17953–17979; b) G. Kresse, D. Joubert, *Phys. Rev. B* **1999**, *59*, 1758–1775.

[20] a) S. Grimme, J. Antony, S. Ehrlich, H. Krieg, *J. Chem. Phys.* **2010**, *132*, 154104; b) S. Grimme, S. Ehrlich, L. Goerigk, *J. Comput. Chem.* **2011**, *32*, 1456–1465.

[21] G. Mills, H. Jónsson, G. K. Schenter, *Surf. Sci.* **1995**, *324*, 305–337.

[22] a) W. Tang, E. Sanville, G. Henkelman, *J. Phys.: Condens. Matter* **2009**, *21*, 084204; b) E. Sanville, S. D. Kenny, R. Smith, G. Henkelman, *J. Comp. Chem.* **2007**, *28*, 899–908; c) G. Henkelman, A. Arnaldsson, H. Jónsson, *Comput. Mater. Sci.* **2006**, *36*, 254–360; d) M. Yu, D. R. Trinkle, *J. Chem. Phys.* **2011**, *134*, 064111.

[23] a) J. Heyd, G. E. Scuseria, M. Ernzerhof, *J. Chem. Phys.* **2003**, *118*, 8207–8215; b) J. Heyd, G. E. Scuseria, *J. Chem. Phys.* **2004**, *121*, 1187–1192; c) J. Heyd, G. E. Scuseria, M. Ernzerhof, *J. Chem. Phys.* **2006**, *124*, 219906.

[24] a) G. Kresse, J. Hafner, *Phys. Rev. B* **1993**, *47*, 558–561; b) G. Kresse, J. Hafner, *Phys. Rev. B* **1994**, *49*, 14251–14269; c) G. Kresse, J. Furthmüller, *Phys. Rev. B* **1996**, *54*, 11169–11186; d) G. Kresse, J. Furthmüller, *Comput. Mat. Sci.* **1996**, *6*, 15–50.

[25] A. A. Peterson, F. Abild-Pedersen, F. Studt, J. Rossmeisl, J. K. Nørskov, *Energy Environ. Sci.* **2010**, *3*, 1311–1315.

[26] T. V. Harris, R. K. Szilagyi, *Inorg. Chem.* **2011**, *50*, 4811–4824.

[27] E. D. Glendening, J. K. Badenhoop, A. E. Reed, J. E. Carpenter, J. A. Bohmann, C. M. Morales, C. R. Landis, F. Weinhold, NBO6.0, Theoretical Chemistry Institute, University of Wisconsin, Madison, USA, 2013.

[28] L. M. Azofra, N. Li, D. R. MacFarlane, C. Sun, *Energy Environ. Sci.* **2016**, *9*, 2545–2549.

[29] W. H. Koppenol, J. D. Rush, *J. Phys. Chem.* **1987**, *91*, 4429–4430.

[30] J. H. Montoya, C. Tsai, A. Vojvodic, J. K. Nørskov, *ChemSusChem* **2015**, *8*, 2180–2186.

Table of Contents

FULL PAPER

Mild conditions N_2 capture and catalytic conversion into NH_3 is a key priority for 'green fuels' technology. Our DFT findings show that Fe-deposited-on MoS_2 2D sheet selectively captures N_2 gas and convert N_2 into NH_3 with maximum energy input of 1.02 eV that arises from the activation barrier for the first H^+/e^- pair transfer

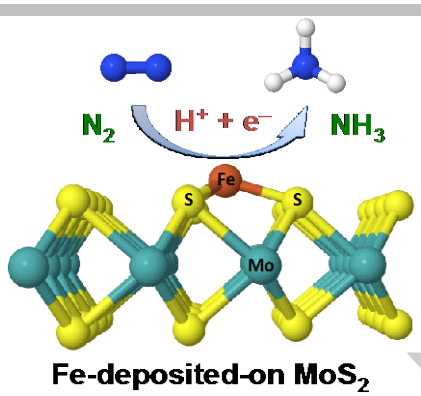

Fe-deposited-on MoS_2

L. M. Azofra, C. Sun, L. Cavallo, D. R. MacFarlane**

Page No. XXXX – Page No. XXXX

Feasibility of N_2 binding and reduction into ammonia at Fe-deposited-on MoS_2 2D sheets: A DFT study